Journal of Cancer Research and Clinical Oncology (2024) 150:492
https://doi.org/10.1007/s00432-024-06016-6

RESEARCH

Transformation zone at the vallate papillae: a significant source of papillomavirus infection at the base of the tongue?

Bosen Zhou[1,2,3,4] · Dan Li[5] · Xinyu Chen[1,2,3,4] · Fangzhou Cai[5] · Jiarui Cui[5] · Siyu Liu[1,2,3,4] · Wei Wang[5] · Dahai Yu[6]

Received: 27 September 2024 / Accepted: 24 October 2024

Abstract

Objective The aim of this study was to investigate whether the base of the tongue harbours a transformation zone (TZ), i.e., an initiation site for papillomavirus infection, analogous to that in the uterine cervix by examining the histological structure of Von Ebner's gland ducts in the vallate papillae.

Methods Immunohistochemical staining and immunofluorescence techniques were used to detect markers associated with the uterine cervical TZ in the vallate papillae, and these results were compared with those in uterine cervical tissue. Additionally, tongue samples from mouse papillomavirus (MmuPV1)-infected mice were analysed to test our hypothesis.

Results The specific expression of CK17 in the squamous epithelium of the vallate papillae indicated the presence of immature squamous epithelium, arising from the transformation of reserve cells in this region. Moreover, a s determined using virus-infected mice, the TZ at the base of the tongue was a significant site for papilloma virus infection.

Conclusions This is the first study to reveal the presence of a TZ in the vallate papillae, as determined by the presence of reserve cells and immature squamous epithelium, suggesting that the base of the tongue is a significant site for papillomavirus infection. This finding provides an entry point for the early prevention and diagnosis of HPV-associated lesions in the oropharynx.

Keywords Transformation zone (TZ) · Papillomavirus · Vallate papillae · Base of tongue · Squamous−columnar junction (SCJ)

Introduction

The incidence of oropharyngeal carcinoma is increasing, and oropharyngeal carcinoma has become the most prevalent squamous head and neck carcinoma in some parts of the world. Currently, the incidence of oropharyngeal carcinoma

Bosen Zhou and Dan Li have contributed equally to this work.

✉ Wei Wang
wangw@cnilas.org

✉ Dahai Yu
yudahai813@sr.gxmu.edu.cn

[1] College of Stomatology, Guangxi Medical University, Nanning 530021, China

[2] Guangxi Key Laboratory of Oral and Maxillofacial Rehabilitation and Reconstruction, Nanning 530021, China

[3] Guangxi Clinical Research Center for Craniofacial Deformity, Nanning 530021, China

[4] Guangxi Health Commission Key Laboratory of Prevention and Treatment for Oral Infectious Diseases, Nanning 530021, China

[5] National Center of Technology Innovation for animal model. National Human Diseases Animal Model Resource Center. Key Laboratory of Pathogen Infection Prevention and Control (Peking Union Medical College), Ministry of Education. NHC Key Laboratory of Comparative Medicine. Institute of Laboratory Animal Science, CAMS & PUMC, Beijing 100020, China

[6] First Affiliated Hospital of Guangxi Medical University, Nanning 530021, China

Published online: 11 November 2024

continues to increase significantly at a rate of 3% per year (Porceddu et al. 2024; Zumsteg et al. 2023). In certain European countries, the incidence of oropharyngeal carcinoma has tripled over the past three decades (Lehtinen et al. 2021). Although traditional risk factors for oropharyngeal carcinoma include smoking and alcohol consumption, this surge is largely attributed to the increasing incidence of human papillomavirus (HPV) infection. In the United States, the incidence and healthcare burden of HPV-associated oropharyngeal carcinoma have surpassed those of HPV-related uterine cervical carcinoma (Dorta-Estremera et al. 2019). To conduct in-depth research on the pathogenesis of oropharyngeal carcinoma, we must further understand the mechanisms related to HPV infection in the oropharynx.

Oropharyngeal carcinoma predominantly manifests in specific locations, such as the base of the tongue, tonsils, and soft palate, with squamous cell carcinoma being the most common histological type (Marur et al. 2010). Uterine cervical carcinoma frequently arises following HPV infection, with infectious sites and precursor lesions primarily developing in the transformation zone (TZ) of the uterine cervix. This region, characterized by the replacement of columnar cells with squamous epithelial cells, is established through the interaction of these two cell types at the squamous−columnar junction (SCJ). This process, known as squamous metaplasia, occurs adjacent to the SCJ (Liao and Manetta 1993; Mukonoweshuro et al. 2005; Reich et al. 2017). Squamous metaplasia is believed to originate from uterine cervical reserve cells, which are located beneath the columnar cells of the endocervical epithelium. During sexual maturity, the displaced columnar epithelium is gradually replaced by immature/mature squamous epithelium differentiated from reserve cells, establishing a physiological SCJ in which displacement occurs. The TZ is defined as the area between the original and postpubertal physiological SCJs (Martens et al. 2009; Doorbar and Griffin 2019). Our previous research revealed an SCJ region at the interface of the squamous and columnar epithelium near Von Ebner's gland ducts at the base of the vallate papillae in healthy humans. This region is akin to that found in the SCJ of the uterine cervix. The SCJ area is also hypothesized to be a critical origin for base of tongue carcinoma (Chen et al. 2022; Jach et al. 2021). The presence of an SCJ may indicate the presence of a TZ similar to uterine cervical squamous metaplasia at Von Ebner's gland ducts in the vallate papillae, potentially serving as a predisposition site for HPV infection.

Previous studies using nude mouse models infected with mouse papillomavirus (MumPv1) revealed that papillomavirus-associated carcinoma mostly occurs at the circumvallate region (equivalent to a human vallate papillae) (Cladel et al. 2016). However, the specific reason why papillomavirus-associated carcinoma in mice is confined to the circumvallate papillae region remains unclear. Importantly, papillomavirus infection experiments in mice have focused more on tumorigenesis and ignored early viral infection sites in the oropharynx. We speculate that the presence of TZ structures in the circumvallate papillae region of mice makes this region a susceptible site for papillomavirus infection prior to the development of lesions and, subsequently, a susceptible area for the associated carcinoma. Those possibilities need to be explored in-depth.

In studies of uterine cervical squamous metaplasia, cytokeratin 17 (CK17) is intracellularly expressed in immature squamous metaplasia of the uterine cervix, with its expression decreasing as squamous cells mature, ultimately becoming confined to basal cells upon full maturation into the squamous epithelium. Thus, CK17 is involved in the transition from immature to mature squamous metaplasia (Nilsson et al. 1983; Smedts et al. 1992; Ross et al. 1986). Nilsson and Smedts suggested that CK17 is expressed in uterine cervical reserve cells and that CK17 and p63 containing can be used to identify these cells (Martens et al. 2004). CK7, a marker for columnar epithelial cells, cytokeratin 5 (CK5), a marker for squamous epithelial cells, and anterior gradient protein 2 homologue (AGR2) are also important markers for squamous metaplasia (Jiang et al. 2017). On the basis of the findings of previous studies, we tentatively speculate that CK7, CK5, and AGR2 are potential markers of the TZ at the vallate papillae.

In this study, we initially identified the presence of a TZ at the vallate papillae by observing the vallate papillae with a focus on reserve cells and immature squamous epithelium and preliminarily elucidated the histological features of the vallate papillae TZ. Furthermore, because the deeper anatomical site and more complex physiological environment of the human oropharynx result in the inability to detect viral infection in the oropharynx and because of the impossibility of obtaining oropharyngeal tissue samples at the viral infection stage, the initial papillomavirus infection site in the oropharynx was investigated using MmuPV1-infected animals. Moreover, the TZ was used as a basis for a preliminary discussion of the histological mechanisms of early HPV infection in the vallate papillae.

Materials and methods

General data collection

Vallate papillae and uterine cervix specimens preserved at the Department of Pathology, First Affiliated Hospital of Guangxi Medical University, were collected between 2020 and 2023. Ten formalin-fixed and paraffin-embedded (FFPE) samples of normal vallate papillae derived from tissues adjacent to surgically excised tongue squamous cell carcinoma were obtained. The age of the patients

ranged from 31 to 79 years, with an average of 56.5 years; 6 patients were male, and 4 patients were female. Additionally, five FFPE samples of normal uterine cervix were obtained from hysterotomy samples from patients with heterotopic endometriosis or multiple uterine fibroids; the ages of the patients ranged from 35 to 48 years, with an average age of 41.4 years. All the human vallate papillae and human uterine cervix specimens were re-evaluated by two pathologists to ensure the absence of abnormal epithelial proliferation and intraepithelial lesions. All patients included in the study provided follow-up data. None of the patients had received radiotherapy, chemotherapy or biotherapy before surgery.

Haematoxylin−eosin (H&E), immunohistochemically, immunofluorescence, and in situ hybridization staining results were scrutinized and validated for research by at least two expert pathologists after receiving approval from the Ethics Committee of Guangxi Medical University (Approval No. 2024-E208-01).

Viral infection of mice

Six- to eight-week-old Crl:NU-Foxn1^{nu} mice were obtained from Beijing Vital River Laboratory Animal Technology Co., Ltd. (Beijing, China). All the mice were anaesthetized with tribromoethanol (300 mg/kg). The methods used for the preparation and quantification of the viral inoculum can be found in previous studies (Hu et al. 2015). The tip of the tongue was gently wounded with a 27-gauge needle, and the mice were allowed to recover overnight. The following day, each mouse was again anaesthetized, and the virus inoculum (10 µl of viral stock solution in saline, 1.5×10^8 viral genome equivalents) was placed onto the prewounded sites with additional gentle abrasion with a plastic pipette tip.

To demonstrate the validity of the MmupvPV1 infection experiment, we used Quantitative-Polymerase Chain Reaction (Q-PCR) analysis and monitored the viral load in oral swabs from infected animals at 2, 4, and 6 weeks after infection. Then, a small plastic brush dipped in saline was placed into the mouth, swirled several times, withdrawn and placed into a collection tube for DNA extraction.

A total of nine nude mice were used for this experiment and euthanized after the sixth week of infection. Tissues were then collected, fixed in 4% paraformaldehyde for 24 h, switched to 70% ethanol for 24 h, processed, embedded in paraffin, and sectioned (5 µm thick). Every 10th section was stained with H&E. All animal experiments were conducted following the guidelines approved by the Institutional Animal Care and Use Committee (IACUC) of the Institute of Laboratory Animal Science, Chinese Academy of Medical Sciences (Approval No. WW21002).

Viral load assessments

Oral swabs containing oral cells and saliva were placed in PBS. For DNA extraction, 5 µL of filtered virus mixture was obtained using a DNeasy Blood & Tissue Kit (Qiagen) following the manufacturer's instructions; RNase-free water served as a negative control. The specific experimental methods used can be found in previous studies (Hu et al. 2015). pMusPV was used to generate a standard curve for qPCR analysis. The primer pairs MmuPV1_E2_1 (5′-GCC CGAAGACAACACCGCCACG-3′) and MmuPV1_E2_2 (5′-CCTCCGCCTCGTCCCCAAAAAATGG-3′) and the probe FAM-TGCCCTTTCAGTGGGTTGAGGACAG-MGB were used. TaqMan™ Gene Expression Master Mix was used for qPCR. Each reaction consisted of a final volume of 20 µL, containing 10 µL of TaqMan™ Gene Expression Master Mix, 1 µL of the MmuPV1_E2_1 primer, 1 µL of the MmuPV1_E2_2 primer, and 0.5 µL of the MmuPV1 E2 probe, 1 µL of template DNA, and 6.5 µL of RNase-free water.

Immunohistochemistry, immunofluorescence and in situ hybridization

Formalin-fixed and paraffin-embedded tissue samples were utilized for immunohistochemical (IHC) analyses. For AGR2 (T55771, 1:150; ABmart, Shanghai, China) staining, sections were deparaffinized, dehydrated, and subjected to antigen retrieval by heating in citrate buffer (pH 6.0) at 121 °C for 30 min, followed by cooling to room temperature. CK17 (bs-1431R, 1:200; Bioss, Beijing, China), CK7 (bs-1610R, 1:200; Bioss, Beijing, China), and CK5 (bs-1060R, 1:200; Bioss, Beijing, China) staining involved similar preparations in Tris (hydroxymethyl) aminomethane-ethylenediaminetetraacetic acid (Tris–EDTA) buffer (pH 9.0). Endogenous peroxidase activity was inhibited via the addition of 3% hydrogen peroxide for 20 min. To avoid nonspecific binding, the sections were incubated overnight at 4 °C with primary antibodies against CK17, CK7, and CK5. The sections were subsequently treated with a secondary antibody (PV6000) for 20 min per the manufacturer's guidelines, with intermittent phosphate-buffered saline rinses. Colour development was achieved using diaminobenzidine, after which the sections were counterstained with haematoxylin.

For immunofluorescence, a Goat Anti-Mouse/Rabbit Multiplex IHC Detection Kit (18003, ZenBio, Chengdu, China) was used following the manufacturer's instructions. The pretreatment steps, including deparaffinization and antigen retrieval, mirrored those used for IHC staining. The following primary antibodies were used: anti-CK17 (bs-1431R, 1:200; Bioss, Beijing, China) and anti-p63 (bsm-52514Rbs-0723R, 1:250; Bioss, Beijing, China). The secondary antibody was goat anti-mouse/rabbit HRP polymer.

Next, the tissue sections were incubated with TSA 520 Dye (enhanced with a TSA Enhancer) for 15 min in the dark. The steps from antigen retrieval to dye incubation were repeated until various tyramine fluorescein substrates were applied. Finally, the sections were counterstained with the nuclear dye DAPI and visualized using an Olympus FV3000 fluorescence microscope.

For in situ hybridization (ISH) staining of mouse tissue sections, we used the RNAscope 2.5 HD Detection Reagents-Brown (322310) and RNAscope Probe-MusPV-E6-E7 probes (409771), which were purchased from Advanced Cell Diagnostics (ACD, Hayward, CA, USA). A horseradish peroxide enzyme-labelled probe and colorimetric readout were used for detection in situ.

Statistical analysis

Categorical variables were expressed as numbers (percentages) and compared using the Fisher's exact test. Continuous variables were expressed as medians (interquartile ranges). All tests were two-sided, with a significant level of $p < 0.05$. All data were analyzed using Statistical Product and Service Solutions (SPSS) 26.0.

Results

H&E staining of human vallate papillae

H&E staining revealed human Von Ebner's glandular ducts at the base of the sulcus and the TZ of the SCJ above it. This region displayed nonkeratinized stratified squamous epithelium, with maturing around the vallate papillae. Notably, Von Ebner's glandular ducts were also observed on the lateral wall of the sulcus (Fig. 1A, B).

Comparison of IHC and IF staining results for the vallate papillae and uterine cervix

CK5 was expressed throughout the squamous epithelium (Fig. 2A, E), whereas CK7 was predominantly found in the columnar epithelium. However, unlike the simple ciliated columnar epithelium at the uterine cervix, pseudostratified ciliated columnar epithelium was present at Von Ebner's glandular ducts (Fig. 2B, F). The SCJ region was characterized by CK5 and CK7 expression at the edges of the vallate papillae and the uterine cervix, with similar expression patterns observed near the SCJ in both locations. Except for taste buds, CK7 expression was largely absent from the squamous epithelium at the region of the vallate papillae, whereas CK5 expression spanned the entire squamous region (Fig. 2A). In contrast, CK7 expression was higher in the superficial layer on the squamous side of the SCJ in the uterine cervix than in the vallate papillae. CK7 was intensely expressed in the columnar epithelial area of the SCJ in both the vallate papillae and the uterine cervix (Fig. 2B, F). Since simple ciliated columnar epithelium is present in the uterine cervix, CK5 was not detected in the basal layer of the columnar epithelium in the uterine cervix (Fig. 2E), but CK5 was intensely expressed in the basal layer of the pseudostratified ciliated columnar epithelium in the vallate papillae (Fig. 2A), suggesting a possible trend towards squamous metaplasia of the columnar epithelium.

CK17 expression was localized to the cytoplasm. Above the SCJ region, a zone of CK17-positive nonkeratinized squamous epithelium extended to the apex of the vallate papillae and the surrounding squamous epithelium (Fig. 2C). The expression of AGR2, a marker of secretory function, was similar to that of CK17 above the SCJ region, suggesting that some columnar epithelial secretory functions are preserved in CK17-expressing immature squamous epithelia (Fig. 2D). In mature squamous epithelium outside the vallate

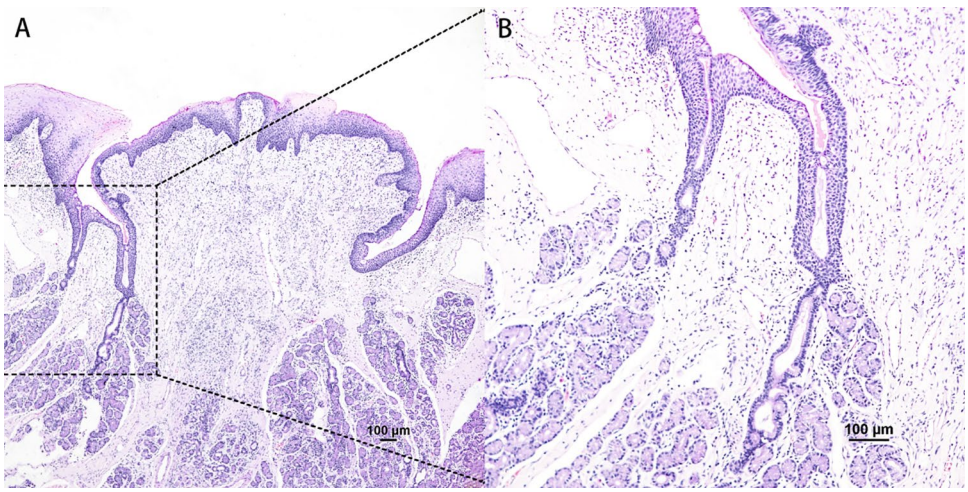

Fig. 1 Normal human vallate papillae. H&E staining of the vallate papilla; **A** ×4; **B** ×10

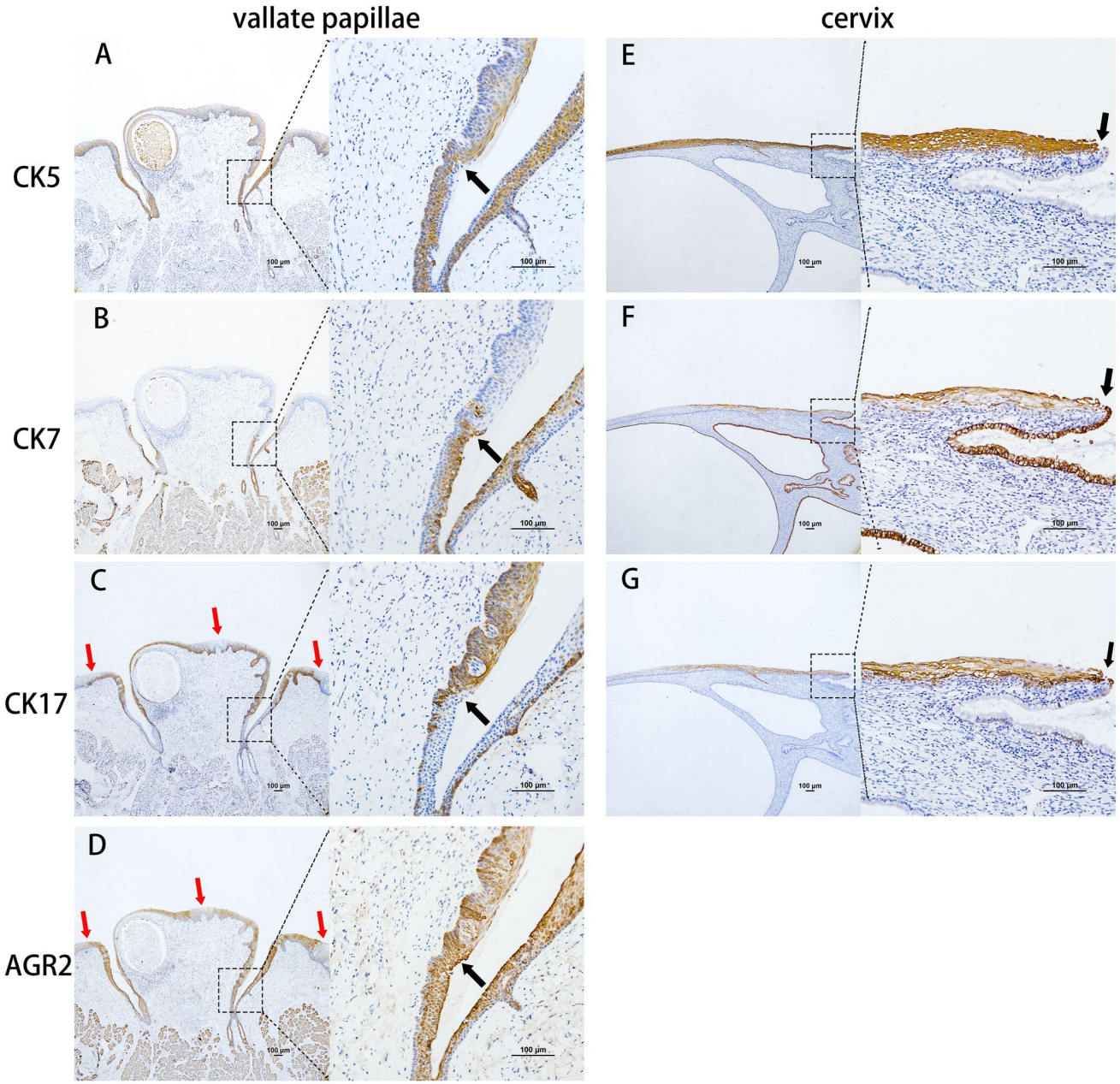

Fig. 2 The distribution and histological characteristics of the epithelial transformation zone in normal human vallate papillae and uterine cervix were examined via immunohistochemistry. Red arrows denote the localization of CK17 and AGR2 in the vallate papillae. The black arrows indicate the SCJ. CK5 IHC staining of the vallate papillae and uterine cervix; **A** ×4 and ×20; **E** ×4 and ×20. CK7 IHC staining of the vallate papillae and uterine cervix; **B** ×4 and ×20; **F** ×4 and ×20. CK17 IHC staining of the vallate papillae and uterine cervix; **C** ×4 and ×20; **G** ×4 and ×20. **D** AGR2 IHC staining of the vallate papillae; ×4 and ×20

papillae, CK17 expression was either absent or sporadically present in basal cells. Notably, the CK17 expression pattern adjacent to the SCJ region in both the uterine cervix and vallate papillae was basically similar: in the columnar epithelium near the SCJ, CK17 was predominantly expressed in basal epithelial cells, with the number of CK17-positive basal cells decreasing with increasing distance from the SCJ region (Fig. 2C, G). Similarly, in both the uterine cervix and vallate papillae, CK17-positive immature squamous epithelium gradually disappeared at a certain distance from the SCJ area, representing further differentiation of immature squamous epithelium to mature squamous epithelium (Fig. 2E, F).

Concurrent CK17 and p63 expression beneath the columnar epithelium was used to identify reserve cells, with CK17/p63 coexpression in basal cells designating

them as reserve cells. Double immunofluorescence localization was used to precisely delineate the distribution of reserve cells (Fig. 3A, B), following the assessment of the immunohistochemical staining results for CK17 and p63 in the vallate papillae. For immunofluorescence staining, p63 was used to stain cell nuclei red, and CK17 was used to stain cytoplasm green. Both immunohistochemistry and immunofluorescence staining revealed reserve cells concentrated in the basal layer of the columnar epithelium near the SCJ region (Fig. 3C–F). Compared with previous studies (Regauer and Reich 2021), the distribution characteristics of reserve cells in the SCJ area of the vallate papillae were similar to those of the uterine cervix.

Viral detection in the oral cavity

We identified MmuPV1 in oral swabs at 2 weeks post infection, marking the earliest time point at which we conducted tests to minimize the risk of interference with viral establishment (Wang et al. 2023). As seen in Table 1, the MmuPV1 copy number was consistently detectable in oral swabs from all infected mice 2 weeks post infection. When MmuPV1 infection was established in all the animals, we consistently observed a significantly greater MmuPV1 copy number until 6 weeks after infection (Fig. 4).

Observation of MmuPV1-infected sites in mouse circumvallate papillae

After 6 weeks of MmuPv1 infection in the mouse oral cavity, no visible anomalous lesions had developed in the

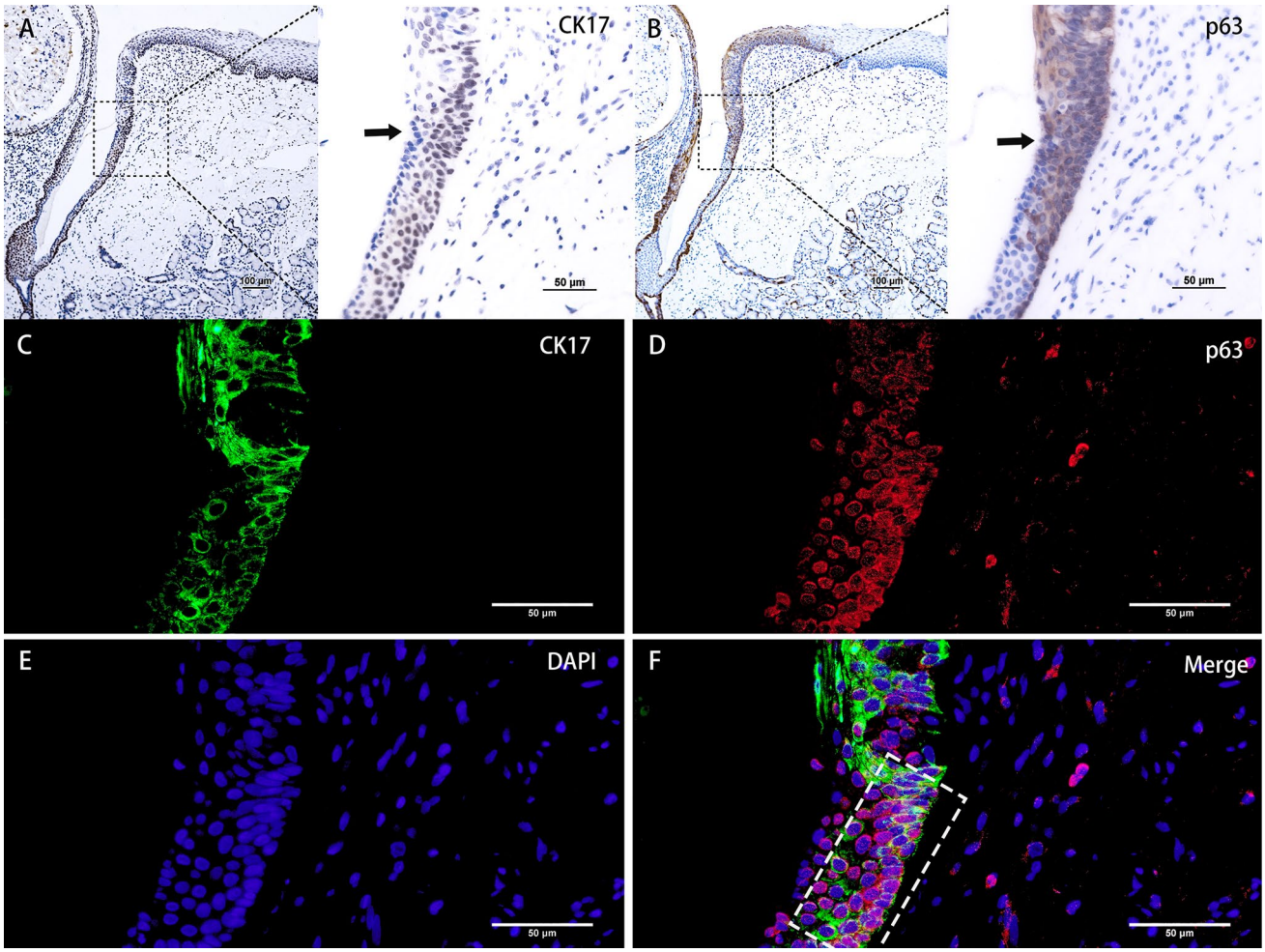

Fig. 3 Distribution of reserve cells in normal human vallate papillae. The distribution range of reserve cells within the white dashed line; black arrows indicate the SCJ. **A** p63 IHC staining for the SCJ at the vallate papilla, ×10 and ×40. **B** CK17 IHC staining for the SCJ at the vallate papilla, ×10 and ×40. **C** CK17 IF staining for the SCJ at the vallate papilla, ×40. **D** p63 IF staining for the SCJ at the vallate papilla, ×40. **E** DAPI IF staining for SCJ at the vallate papilla, ×40. **F** merged p63 and CK17 IF staining of reserve cells, ×40

Table 1 Viral DNA in nude mice infected with MmuPV1 in the oral cavity and oropharynx was tracked

	Mouse 1	Mouse 2	Mouse 3	Mouse 4	Mouse 5	Mouse 6	Mouse 7	Mouse 8	Mouse 9
Week 2	4.07×10^6	3.65×10^5	1.24×10^6	1.48×10^6	5.14×10^6	3.48×10^5	2.87×10^5	4.15×10^5	3.36×10^6
Week 4	3.50×10^6	3.78×10^6	8.43×10^5	1.59×10^6	6.05×10^6	4.43×10^5	3.00×10^6	4.55×10^5	4.25×10^6
Week 6	4.59×10^6	5.91×10^6	1.96×10^6	2.61×10^6	9.58×10^6	9.60×10^5	5.56×10^6	9.23×10^5	7.25×10^6

The viral DNA load in the oral cavity/oropharynx over time was determined by qPCR analysis (viral copy numbers/μL)

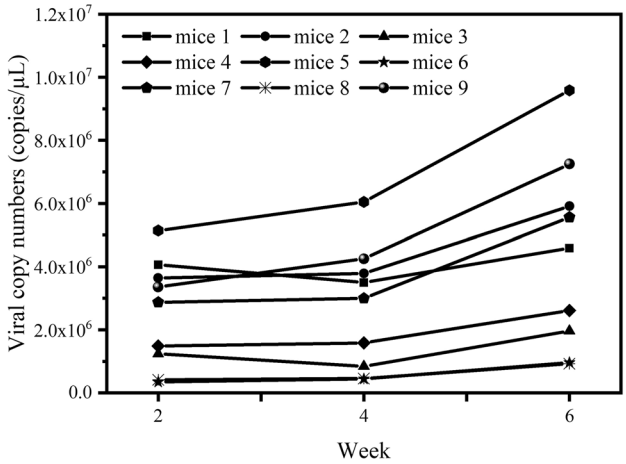

Fig. 4 Viral load (qPCR) in the MmuPV1-infected oral cavity/oropharynx

tongue, and the colour, morphology, and texture of the tongue remained unchanged, suggesting that papillomavirus-associated lesions had not yet developed in the oropharynx or entire tongue of the mice during this stage. The virus-infected wound areas healed (Fig. 5A). The ISH results revealed that, except the wounded site, MmuPV1 infection was restricted to the circumvallate papillae in almost all the mice tested, with virtually no virus-infected cells detected in the middle dorsal tongue, the ventral tongue, or the base of the tongue behind the circumvallate papillae. In a portion of the test mice, MmuPV1-E6-E7 RNA-positive cells were observed in the circumvallate papillae even when no virus-infected cells were found at the wound site coated with virus (Fig. 5C).

Fisher's test revealed that the MmuPV1-positive infection rates in the circumvallate papillae were greater than those in other areas ($p=0.001$) (Table 2). Further pairwise comparisons of the MmuPV1-positive infection rates at different tongue sites were performed. The results revealed that the MmuPV1-positive infection rates in the circumvallate papillae group were significantly greater than those in the middle dorsal tongue or ventral tongue groups ($p=0.015$). Thus, in the early stages of infection, the circumvallate papillae is a susceptibility site for papillomavirus infection.

In our previous study, the presence of an SCJ area in the mouse/rat circumvallate papillae similar to that of humans was demonstrated by histology, and the physiology of this

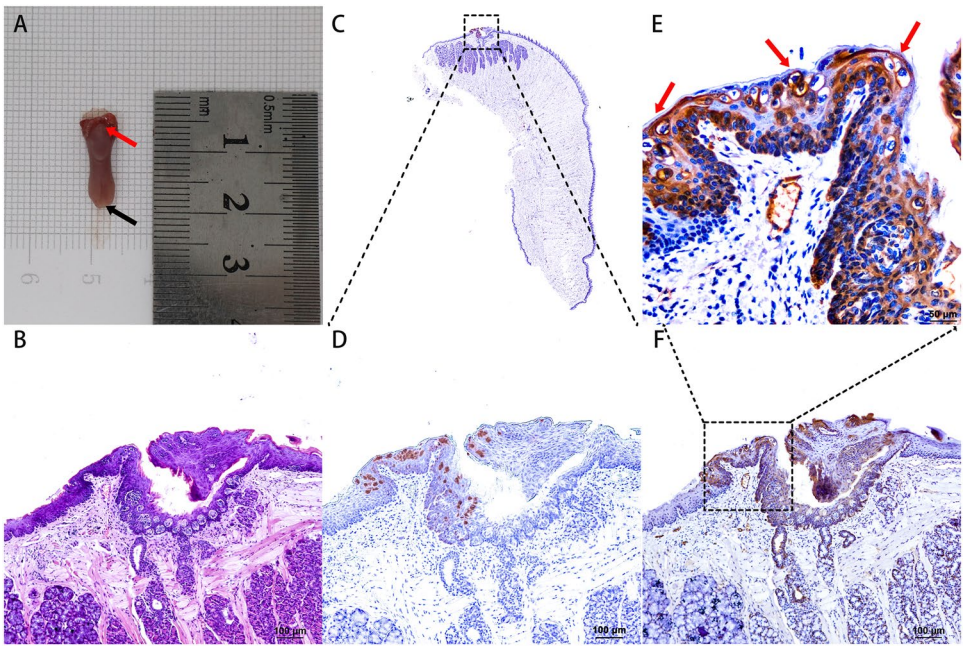

Fig. 5 Tongue morphology, ISH and IHC staining of tongue tissue from nude mice after 6 weeks of infection. **A** Tongues of infected mice; red arrows denote circumvallate papillae; black arrows denote virus-coated areas. **B** H&E staining of the circumvallate papilla, ×10. MmuPV1-E6-E7 ISH staining of the tongues of infected mice; **C** ×1 and **D** ×10. CK17 IHC staining of the circumvallate papilla; red arrows indicate the distribution of koilocytotic cells; **E** ×20 and **F** ×10

Table 2 Differences in the distribution of Mmupv1 infection at different sites in mice based on Fisher's exact test

Site of tongue	*N*		Infection rates (%)	*p* value
	Mmupv1 infection (+)	Mmupv1 infection (−)		
Circumvallate papillae	7	2	77.78	
Middle dorsal tongue	1	8	22.22	
Ventral tongue	1	8	22.22	0.001
Base of the tongue behind the circumvallate papillae	0	9	0	

area was described (Chen et al. 2023). The immature squamous epithelium of the infected mice was observed by the expression of CK17. Immunohistochemical analysis of CK17 revealed that the mouse circumvallate papillae possesses a TZ structure analogous to that of humans. The CK17-positive immature squamous epithelium extended from the base of the circumvallate papillae sulcus to the tongue surface, gradually transitioning to a structurally mature squamous epithelium (Fig. 5F). Koilocytotic cells induced by papillomavirus infection were observed within the CK17-positive immature squamous epithelium but not in the tongue tissue outside the circumvallate papillae TZ (Fig. 5E). H&E staining revealed no epithelial dysplasia or other related lesions in the entire tongue of the mice (Fig. 5B). A comparison of the IHC and ISH results for serial sections revealed that MmuPV1-E6-E7 RNA-positive cells were distributed in the immature squamous epithelium with positive CK17 expression, and no virus-infected cells were observed in the mature epithelium outside the region of the TZ (Fig. 5C, D, F). However, no virus-infected cells were observed within or adjacent to the CK17-expressing reserve cells under the columnar epithelium (Fig. 5D, F).

Discussion

It is widely accepted that most uterine cervix carcinomas and related precancerous lesions tend to develop in a TZ. Conversely, patients with oropharyngeal carcinoma are typically diagnosed at advanced stages because of the absence of early clinical symptoms, insidious progression, and early lymphatic metastasis, resulting in delayed detection (Palmer et al. 2014; Huang et al. 2018). Mestre et al. (2020) reported that squamous carcinoma tends to arise near the circumvallate papillae in both MmuPV1-infected nude mice and K14-HPV16 transgenic mice. Consequently, Mestre et al. (2020) proposed the existence of a TZ at the circumvallate papillae in mice, similar to that in the uterine cervix. However, no studies have investigated the TZ of the oropharynx, making it challenging to predict HPV susceptibility before clinical lesion onset and complicating the diagnosis and treatment of HPV-associated oropharyngeal carcinoma.

This study revealed CK17-labelled immature squamous epithelium on the squamous side of the SCJ zone within the vallate papillae. The expression patterns of AGR2 and CK17 in the squamous epithelium of the vallate papillae region were consistent (Fig. 2C, D). Considering that AGR2 has secretory functions, it is hypothesized that the immature squamous epithelium marked by CK17 retains certain secretory characteristics of the columnar epithelium. The preservation of secretory function implies that the CK17-positive immature squamous epithelium in the vallate papillae region may result from the squamous metaplasia of the columnar epithelium. This finding reinforces the hypothesis that immature squamous epithelium exists in the TZ at the human vallate papillae. The extent of the TZ at the base of the vallate papillae was delineated by comparison with the uterine cervical TZ. Furthermore, the distribution of reserve cells in the SCJ region of the vallate papillae was assessed via CK17/p63 immunofluorescence staining (Fig. 3D, F), which revealed that reserve cells colabelled with CK17/p63 in the vallate papillae area are likely to be the origin of carcinoma (Martens et al. 2009; Zheng et al. 2023). Prior studies have suggested that reserve cells might be target cells for HPV infection in the uterine cervix (Smedts et al. 2008; Reya et al. 2001; Watt 1998).

The characteristics of early papillomavirus infection in the oropharynx remain unknown due to the clinical impossibility of observing the initial viral infection status. Therefore, this study is the first to observe papillomavirus infection at the base of the tongue in MmuPv1-infected mice prior to the occurrence of related lesions. ISH experiments revealed that in a portion of infected mice, virus-infected cells were not present beneath the columnar epithelium near the SCJ but were present in the immature squamous epithelium within the TZ of the vallate papillae (Fig. 5D, F). These findings suggest that papillomavirus infection targets in the vallate papillae region are not limited to reserve cells and that immature squamous epithelium in the TZ of the vallate papillae is more susceptible to early papillomavirus infection. Persistent papillomavirus infection requires the long-term maintenance of viral genomes at low copy numbers in undifferentiated cells of the epithelia (Doorbar et al. 2021). Thus, epithelial damage or unstable epithelial structures are important for the development of papillomavirus infections. The immature squamous epithelium of the vallate papillae TZ, because of its tendency to further differentiate and its simple epithelial structure, as well as the more superficial anatomical location of the immature squamous epithelium, may be susceptible to early papillomavirus infection. Thus, the

vallate papillae becomes a virus-susceptible area, probably because of the histologic structure of the immature squamous epithelium in the vallate papillae TZ.

Reserve cells in the vallate papillae region are less susceptible to papillomavirus infection than those in the cervical region are, probably due to their more cryptic distribution in the vallate papillae. However, during the development of HPV-associated carcinoma, high-risk HPVs are able to influence cell cycle control mechanisms, leading to tumorigenesis (Steenbergen et al. 1996). Thus, HPV-infected target cells associated with oropharyngeal carcinogenesis are likely undifferentiated, multiplying cells, which makes it possible for a virus to incorporate into cellular DNA during the cell cycle. A stem cell can serve as the origin of carcinoma through disturbances in the "asymmetric" division process, thus becoming a target cell of high-risk HPV infection (Martens et al. 2009; Zheng et al. 2023). Theoretically, reserve cells beneath the columnar epithelium of the vallate papillae may possess stem cell properties and thus be risk factors for the development of carcinoma after papillomavirus infection. If reserve cells are infected by the virus, a longer infection time and other stimuli may be needed to reduce local tissue immune function (e.g., MmuPV1 infection combined with 4-nitroquinoline-1-oxide stimulation). This also seems to explain why, in previous studies, simple viral infection does not readily induce carcinoma; additional stimuli must be applied (Wei et al. 2020). Therefore, in the study of papillomavirus-associated carcinoma, infection of the reserve cells of the vallate papillae TZ should be the focus of attention.

Although the TZ formed by squamous metaplasia is recognized as a high-risk area for uterine cervical viral infection due to the aggregation of reserve cells and active cell proliferation, the underlying mechanisms remain unclear. In the SCJ region, a population of reserve cells exists at the basal part of the columnar epithelium. Traditionally, the columnar epithelium is believed to be supplanted by immature chemosynthetic squamous epithelium through the differentiation and proliferation of these reserve cells (Martens et al. 2009; Chumduri et al. 2021). In our study, pronounced CK17 expression was observed at the base of the columnar epithelium adjacent to the SCJ region of the vallate papillae, accompanied by robust reserve cell proliferation, corroborating the traditional view. However, some scholars argue that intermediary cells at the squamous-columnar junction of the uterine cervix are the initial triggers of squamous metaplasia, differentiating into a "reserve cell"-like population from the top, thus forming immature squamous epithelium (Herfs et al. 2012). These debates have focused predominantly on the uterine cervix TZ, and whether the squamous metaplasia mechanism in Von Ebner's gland is analogous to that in the uterine cervix requires further elucidation through lineage tracing, genetic analyses, and additional pertinent studies.

On the basis of the results of animal experiments and histological observations of the TZ, the vallate papillae maybe a target of clinical detection for the early prevention and detection of HPV-associated oropharyngeal diseases in susceptible populations. The vallate papillae is in a more anterior anatomical position than the tonsils are, offering advantages in clinical work. In basic research, the discovery of a TZ at the vallate papillae may enable a more precise exploration of the pathogenesis of HPV-associated oropharyngeal carcinoma. We will expand the case collection of HPV-associated cases of tongue cancer through a multicentre study to further test our hypothesis, and we hope that more scholars will be able to collaborate in this study. In uterine cervix carcinoma research, excision/destruction of the TZ, the new SCJ and columnar endocervical epithelium with all subcolumnar reserve cells capable of metaplasia, may be an effective approach for the prevention and treatment of HPV-associated lesions (Franceschi 2015). The preventive efficacy of related vaccines in HPV-associated oropharyngeal disease also needs to be evaluated. Accordingly, there is a need for a more detailed exploration of the squamous metaplasia mechanism at the base of the tongue for the clinical management, diagnosis, treatment, and prevention of HPV-associated carcinoma and other lesions.

Conclusion

In this study, we identified an early papillomavirus infection site at the base of the tongue and explored the related histological mechanisms in the TZ. However, the infection of reserve cells associated with tumorigenesis is a 'later event', and therefore, with the short infection time in this study, further exploration of the pathogenesis of carcinoma was not possible. The small number of animals and the lack of exploration at the gene level are also limitations of this study. However, we will complete papillomavirus-associated tumorigenic experiments on the basis of the results of this study and explore the risk of pathogenicity of different subtypes of papillomaviruses in the oropharynx in subsequent studies. The vallate papilla, as a sentinel site in the oropharynx, has obvious anatomical advantages in clinical examination and early treatment, and the results of the present study provide a new entry point for the prevention and diagnosis of HPV-associated oropharyngeal diseases. We hope to use the discovery of the vallate papillae TZ as a new direction for subsequent mechanistic studies of HPV-associated oropharyngeal carcinoma.

Acknowledgements The authors gratefully acknowledge the study participants and staff for their invaluable assistance and cooperation throughout the study.

Author contributions Conceptualization, Bosen Zhou, Dan Li, Wei Wang and Dahai Yu; Funding acquisition, Dahai Yu; Investigation, Xinyu Chen, Fangzhou Cai, Jiarui Cui and Siyu Liu; Methodology, Dan Li, Xinyu Chen, Fangzhou Cai, Jiarui Cui and Siyu Liu; Supervision, Wei Wang and Dahai Yu; Writing—original draft, Bosen Zhou; Writing—review & editing, Bosen Zhou, Dan Li, Wei Wang and Dahai Yu. All authors contributed to the article and approved the submitted version.

Funding This research was funded by the Natural Science Foundation of China [Grant No. 81360407] and the Guangxi Natural Science Foundation [Grant No. 2016GXNSFDA380002].

Data availability No datasets were generated or analysed during the current study.

Declarations

Conflict of interest The authors declare no competing interests.

Ethics This study was conducted in accordance with the Declaration of Helsinki and approved by the Ethics Committee of Guangxi Medical University (Approval No. 2024-E208-01) for studies involving humans. The animal study protocol was approved by the Institutional Animal Care and Use Committee (IACUC) of the Institute of Laboratory Animal Science, Chinese Academy of Medical Sciences (Approval No. WW21002), for studies involving animals.

Informed consent Informed consent was not applicable for this study because this study used only normal human tissue samples stored at the pathology department of the hospital, no patient information was obtained, and patient privacy was not violated.

References

Chen PN, Chen XY, Chen GX et al (2022) Squamous-columnar junction of Von Ebner's glands may be a significant origin of squamous cell carcinomas in the base of the tongue. Front Oncol 12:1029404. https://doi.org/10.3389/fonc.2022.1029404

Chen X, Luo L, Chen P et al (2023) Comparative observations on the squamous-columnar junction of Von Ebner's glandular duct at the bottom of vallate papillae in dogs, rats, mice and human. Folia Morphol. https://doi.org/10.5603/fm.96804

Chumduri C, Gurumurthy RK, Berger H et al (2021) Opposing Wnt signals regulate cervical squamocolumnar homeostasis and emergence of metaplasia. Nat Cell Biol 23(2):184–197. https://doi.org/10.1186/s40425-019-0728-4

Cladel NM, Budgeon LR, Balogh KK et al (2016) Mouse papillomavirus MmuPV1 infects oral mucosa and preferentially targets the base of the tongue. Virology 488:73–80. https://doi.org/10.1016/j.virol.2015.10.030

Doorbar J, Griffin H (2019) Refining our understanding of cervical neoplasia and its cellular origins. Papillomavirus Res 7:176–179. https://doi.org/10.1016/j.pvr.2019.04.005

Doorbar J, Zheng K, Aiyenuro A et al (2021) Principles of epithelial homeostasis control during persistent human papillomavirus infection and its deregulation at the cervical transformation zone. Curr Opin Virol 51:96–105. https://doi.org/10.1016/j.coviro.2021.09.014

Dorta-Estremera S, Hegde VL, Slay RB (2019) Targeting interferon signaling and CTLA-4 enhance the therapeutic efficacy of anti-PD-1 immunotherapy in preclinical model of HPV$^+$ oral cancer. J Immunother Cancer 7(1):252. https://doi.org/10.1186/s40425-019-0728-4

Franceschi S (2015) Embryonic cells in the squamous-columnar junction of the cervix: scope for prophylactic ablation? Int J Cancer 136(5):989–990. https://doi.org/10.1002/ijc.29057

Herfs M, Yamamoto Y, Laury A (2012) A discrete population of squamocolumnar junction cells implicated in the pathogenesis of cervical cancer. Proc Natl Acad Sci USA 109(26):10516–10521. https://doi.org/10.1073/pnas.1202684109

Hu J, Budgeon LR, Cladel NM et al (2015) Tracking vaginal, anal and oral infection in a mouse papillomavirus infection model. J Gen Virol 96(12):3554–3565. https://doi.org/10.1099/jgv.0.000295

Huang SH, O'Sullivan B, Waldron J (2018) The current state of biological and clinical implications of human papillomavirus-related oropharyngeal cancer. Semin Radiat Oncol 28(1):17–26. https://doi.org/10.1016/j.semradonc.2017.08.007

Jach D, Cheng Y, Prica F (2021) From development to cancer—an ever-increasing role of AGR2. Am J Cancer Res 11(11):5249–5262

Jiang M, Li H, Zhang Y et al (2017) Transitional basal cells at the squamous-columnar junction generate Barrett's oesophagus. Nature 550(7677):529–533. https://doi.org/10.1038/nature24269

Lehtinen T, Elfström KM, Mäkitie A (2021) Elimination of HPV-associated oropharyngeal cancers in Nordic countries. Prev Med 144:106445. https://doi.org/10.1016/j.semradonc.2017.08.007

Liao SY, Manetta A (1993) Benign and malignant pathology of the cervix, including screening. Curr Opin Obstet Gynecol 5(4):497–503

Martens JE, Arends J, Van der Linden PJ, De Boer BAG, Helmerhorst TJM (2004) Cytokeratin 17 and p63 are markers of the HPV target cell, the cervical stem cell. Anticancer Res 24(2B):771–775

Martens JE, Smedts FM, Ploeger D (2009) Distribution pattern and marker profile show two subpopulations of reserve cells in the endocervical canal. Int J Gynecol Pathol 28(4):381–388

Marur S, D'Souza G, Westra WH (2010) HPV-associated head and neck cancer: a virus-related cancer epidemic. Lancet Oncol 11(8):781–789. https://doi.org/10.1016/S1470-2045(10)70017-6

Mestre VF, Medeiros-Fonseca B, Estêvão D (2020) HPV16 is sufficient to induce squamous cell carcinoma specifically in the tongue base in transgenic mice. J Pathol 251(1):4–11. https://doi.org/10.1002/path.5387

Mukonoweshuro P, Oriowolo A, Smith M (2005) Audit of the histological definition of cervical transformation zone. J Clin Pathol 58(6):671

Nilsson J, Ksiazek T, Heldin CH (1983) Demonstration of stimulatory effects of platelet-derived growth factor on cultivated rat arterial smooth muscle cells. Differences between cells from young and adult animals. Exp Cell Res 145(2):231–237. https://doi.org/10.1016/0014-4827(83)90001-0

Palmer E, Newcombe RG, Green AC (2014) Human papillomavirus infection is rare in nonmalignant tonsil tissue in the UK: implications for tonsil cancer precursor lesions. Int J Cancer 135(10):2437–2443. https://doi.org/10.1002/ijc.28886

Porceddu SV, Negrello T, Rawson N et al (2024) Human papillomavirus associated oropharyngeal cancer now the most common mucosal head and neck cancer in Queensland. J Med Imaging Radiat Oncol 68(4):472–480. https://doi.org/10.1111/1754-9485.13643

Regauer S, Reich O (2021) The origin of human papillomavirus (HPV)—induced cervical squamous cancer. Curr Opin Virol 51:111–118. https://doi.org/10.1016/j.coviro.2021.09.012

Reich O, Regauer S, McCluggage WG (2017) Defining the cervical transformation zone and squamocolumnar junction: Can we reach a common colposcopic and histologic definition? Int J Gynecol Pathol 36(6):517–522. https://doi.org/10.1097/pgp.0000000000000381

Reya T, Morrison SJ, Clarke MF (2001) Stem cells, cancer, and cancer stem cells. Nature 414(6859):105–111. https://doi.org/10.1038/35102167

Ross R, Raines EW, Bowen-Pope DF (1986) The biology of platelet-derived growth factor. Cell 46(2):155–169. https://doi.org/10.1016/0092-8674(86)90733-6

Smedts F, Ramaekers F, Troyanovsky S (1992) Basal-cell keratins in cervical reserve cells and a comparison to their expression in cervical intraepithelial neoplasia. Am J Pathol 140(3):601–612

Smedts F, Ramaekers FC, Hopman AH (2008) CK17 and p16 expression patterns distinguish (atypical) immature squamous metaplasia from high-grade cervical intraepithelial neoplasia. Histopathology 52(4):515–516; author reply 516–517. https://doi.org/10.1111/j.1365-2559.2008.02941.x

Steenbergen RD, Walboomers JM, Meijer CJ (1996) Transition of human papillomavirus type 16 and 18 transfected human foreskin keratinocytes towards immortality: activation of telomerase and allele losses at 3p, 10p, 11q and/or 18q. Oncogene 13(6):1249–1257

Wang W, Spurgeon ME, Pope A et al (2023) Stress keratin 17 and estrogen support viral persistence and modulate the immune environment during cervicovaginal murine papillomavirus infection. Proc Natl Acad Sci USA 120(12):e2214225120. https://doi.org/10.1073/pnas.2214225120

Watt FM (1998) Epidermal stem cells: markers, patterning and the control of stem cell fate. Philos Trans R Soc Lond B Biol Sci 353(1370):831–837. https://doi.org/10.1098/rstb.1998.0247

Wei T, Buehler D, Ward-Shaw E et al (2020) An infection-based murine model for papillomavirus-associated head and neck cancer. Mbio 11(3):e00908-20. https://doi.org/10.1128/mbio.00908-20

Zheng Y, Liu J, Beeraka NM et al (2023) Inflammation and stem cell stochasticity of HPV-induced cervical cancer: epigenetics based biomarkers through microbiome and metabolome for personalized medicine: a systematic review. Curr Med Chem. https://doi.org/10.2174/0109298673257429231108072717

Zumsteg ZS, Luu M, Rosenberg PS et al (2023) Global epidemiologic patterns of oropharyngeal cancer incidence trends. J Natl Cancer Inst 115(12):1544–1554. https://doi.org/10.1093/jnci/djad169